Improvement on mechanical property of boron carbide reinforced aluminum composites through controlled interfacial reaction

Qing Ruan[a], Yuzhen Jia[b], Jiyun Zheng[b,*], Qiulin Li[c,*], Wei Liu[a], Guogang Shu[c]

[a]School of Materials Science and Engineering, Tsinghua University, Beijing 100084, China

[b]Science and Technolog on Reactor Fuel and Materials Laboratory, Nuclear Power Institute of China, Chengdu, 610041, China

[c]Graduate School at Shenzhen, Tsinghua University, Shenzhen 518055, China

Abstract

A fine bonded interface is essential for the property of metal matrix composites. In this paper, an innovative approach to strengthening boron carbide reinforced aluminum composites (B_4C/Al composites) was proposed and studied by the use of liquid stirring technology. The effect of interfacial reaction on the microstructure and mechanical behavior of B_4C/Al composites was revealed by the addition of Ti element. Through controlled matrix-reinforcement interfacial reaction, a dense and continuous nanoscale layer of TiB_2 was found to be formed on the surface of reinforcement B_4C particles, which also resulted in interfacial modification. Interface modification influenced the mechanical properties through changing interfacial microstructure. Due to the formation of TiB_2 layer with good bonding, interface defects were eliminated. Increasing the degree of modification, such as increasing Ti content and reaction time, the strength of B_4C/Al composites was gradually improved. Severe interfacial reaction also introduced lots of nano-scale TiB_2 particles into the matrix, which influenced the mechanical property. Fracture behavior of B_4C/Al composites with different interfacial modification was deeply discussed at last.

Keywords: Metal matrix composites; Boron carbide; Interfacial reaction; Mechanical property.

*Corresponding author.

Tel./fax: +8602885906082 (Jiyun Zheng), +0086075526036424 (Qiulin Li).

E-mail addresses: zhengjiyun@aliyun.com (Jiyun Zheng), liql@sz.tsinghua.edu.cn (Qiulin Li).

Introduction

In recent years, boron carbide reinforced aluminum composites (B_4C/Al composites) have been widely applied in nuclear power industry for spent fuels transportation and storage, due to the excellent neutron absorption ability of B^{10} atom [1-3]. Basically, there are two kinds of storage systems for spent fuels: wet storage and dry storage. Since it is more flexible and cost-saving than the wet storage, dry storage technology attracts more and more interest for spent fuel treatment. However, in the service environment of dry condition, the neutron absorber materials-B_4C/Al composites-are subjected to elevated temperature during 300-400 ℃ for long periods of time, in addition to high level of gamma radiation and low level of neutron radiation [4]. Researchers have expected to design B_4C/Al composites as either functional or structural neutron absorber materials. Therefore, such severe conditions have highlighted the demand for mechanical property of B_4C/Al composites.

There are many factors that influence the mechanical behavior of particle reinforced metal matrix composites (MMCs), such as volume fraction of reinforcement, particle size, inter-particle distance, surface microstructure of reinforcement, and interfacial bonding state [5-8]. Under an applied load, the load is transferred from the weaker matrix, across the matrix/reinforcement interface, to the typically higher stiffness reinforcement. Besides, thermally-induced dislocations intend to form at the interface due to the thermal mismatch between reinforcement and matrix [9]. A strong interface will usually allow for effective load transfer from the matrix to the reinforcement, leading to improved strength, stiffness and resistance to environmental attack [10]. H. Zhang et.al investigated the effect of interface damage on constitutive behavior of particle reinforced metal matrix composites and found that imperfect interface microstructure resulted in decreased flow strength and the failure strain [11]. As special for B_4C/Al composites, weak interface bonding leaded to interfacial debonding dominated fracture behavior [12]. L. M. Tham et.al prepared SiC/Al composites with two distinct interfacial microstructures through

controlled interface reaction [13, 14]. They found that the formation of a thin Al_4C_3 reaction layer along particle–matrix interface helped to overall improve material's mechanical behavior such as yield strength, ultimate tensile strength, work-hardening rate and work-to-fracture, and also changed the fracture pattern from one involving interfacial decohesion to one where particle breakage was dominant. Therefore, a good bonding interface is essential for the property of metal matrix composite materials.

In fact, when metal matrix composites are produced by molten metal methods, the reaction between reinforcements and molten metal has to be serious considered, which directly influences interfacial microstructure and thus mechanical behavior [15]. Previous researches [16, 17] have revealed a common interfacial reaction occurred in stirring-casted B_4C/Al composites, as expression (1):

$$9Al(l) + 2B_4C = 2Al_3BC + 3AlB_2 \quad (1)$$

Since above reaction is much severe and then decreases the fluidity of composites melt, Ti element is chosen to add into the melt to suppress original interfacial reaction and the reaction is changed to be expression (2) [18-20]:

$$6Al(l) + 2B_4C + 4Ti = 2Al_3BC + 3TiB_2 \quad (2)$$

AlB_2 is replaced by newly formed TiB_2 layer, which tightly surrounds the B_4C particles and reduces the rate of particle degradation as a protective layer, which also leads to the transformation of interfacial microstructure from rough surface to smooth interface with fine TiB_2 layer and dispersively distributed large TiB_2 crystals. The thickness of fine TiB_2 layer can be small to less than 1 μm, even tens of nanometers. It is believed that interfacial reaction layers with nano-level thickness are thought to be beneficial to mechanical properties since they usually enhance both the chemical and mechanical bonding between the particle and the matrix [21]. A.R. Kennedy tested the mechanical properties of casted B_4C/Al composites and revealed that increased adhesion could be achieved by Ti-B-C reaction layer considering its higher stiffness and modulus [22]. Although it is accepted that chemical interface with coherency or

semicoherency improves load transfer and hence favors good mechanical properties [23], previous researches don't deeply investigate the inner relationship between interfacial reaction and mechanical behavior of B_4C/Al composites with addition of Ti, especially rarely focus on how to improve the mechanical property by artificially adjusting interfacial microstructure. Besides, due to strong stirring and growth stress, we found that those large TiB_2 crystals at the interface tended to fall apart from particle surface into aluminium matrix in our previous article [18]. These TiB_2 slices are in-site second reinforcement with size of nanometers, whereas the effect of second TiB_2 slices on mechanical property and fracture behavior of B_4C/Al composites is not clear.

In this study, the effect of matrix-reinforcement interfacial reaction on mechanical property of B_4C/Al composites with additional Ti element is investigated under the objective of improving tensile and fracture behavior by modification on interfacial microstructure, which is achieved through controlled interfacial reaction. It is expected to figure out the proper extent of interfacial reaction and optimal interfacial microstructure in this system of B_4C/Al composites. Thus, as neutron absorber materials, B_4C/Al composites with optimal combination of mechanical property and neuron shielding ability will satisfy the requirement of dry storage and transportation application of spent fuels.

Experimental

To generate different interfacial microstructure, four batches of B_4C/Al composites billets were prepared by varying the Ti content and stirring time. The amount of Ti element and stirring time are shown in table 1. The preparation procedure of B_4C/Al composites by stirring-casting method was as follows: commercially pure Al and Al-Ti master alloy were first melt in a stirring-casting furnace under vacuum condition ($<$10 Pa). The temperature was kept at 730 ℃ after long time holding. B_4C powders with average diameter D[4,3] = 24.937 μm and span of size distribution λ = 1.34 were added into the melt [24]. Masses of all materials

were designed for B_4C/Al composites consisting of 15 wt.% B_4C and corresponding Ti content. In the following part, IDs C0.5, C1, C1.5 and C2.5 are used to represent four composites with Ti content of 0.5, 1, 1.5 and 2.5 (in wt.%), respectively. A mechanical stirrer was used to incorporate B_4C particles through agitating the melt. Stirring speed was constant at 500 rpm/min to form stable vortex. A transition period less than 5 min was necessary for total entrance of B_4C particles. Once stirring time was reached, the melt was directly casted into a preheated rectangle mould with 420 ℃. The whole stirring and casting process was under protective atmosphere of argon for avoiding oxidation. To eliminate the casting defects and improve uniform distribution of reinforcements, as-manufactured B_4C/Al billets with size of 20×30×50 mm were hot rolled at 450 ℃ to a final sheet thickness of 1 mm. Subsequently B_4C/Al composites sheets were annealed at 370 ℃ to obtain recrystallized grain matrix.

To characterize the microstructure of B_4C/Al composites, ion beam (IB-09020CP, JEOL) and mechanical polishing methods were used to process samples. Mechanical polishing was down to 1 μm by using diamond suspension. A scanning electron microscopy (SEM, TESCAN MIRA 3 LMH), in back scattered electron (BSE) mode, equipped with Energy Dispersive Spectrometer (EDS) and Electron Backscattered Diffraction (EBSD), was used to observe the interface and matrix microstructure. Tensile tests to failure were performed at room temperature using an universal tensile machine in accord to ISO 6892-1: 2009. The moving speed of fixed side was constant at 0.5 mm/min during the whole test. Fig. 1 shows the size of tensile specimens. The offset yield strength (0.2%) and ultimate tensile strength were calculated from the load versus elongation data, which was recorded by an extensometer attached to the test specimen. Then the fracture surface of failed specimens was observed by SEM to analyze the failure mechanisms of B_4C/Al composites under tensile loading.

Results and discussion

To investigate the influence of interface structure on the mechanical property of

B_4C/Al composites, uniform distribution of B_4C particles is necessary to eliminate the effect of particles distribution on the mechanical property, especially B_4C clusters. Fig. 2 presents the B_4C particle distribution of B_4C/Al composites under different preparation conditions. Uniform distribution of B_4C particles is obtained in each aluminum matrix, although some minor difference exists. Thus it can be assumed that the distribution of B_4C particles in all composites is similar and the influence of B_4C particle distribution on mechanical property could be ignored in following discussion. Besides, the grain size of aluminum matrix and residual deformation stress can also influence the tensile behavior of B_4C/Al composites. In order to eliminate the effect of hot rolling, all sheets were recrystallized by annealing treatment at 370 ℃ for 1 h. As shown in Fig. 3, the grains of B_4C/Al composites transformed to equiaxial grain and grain size approximately equals in each composites matrix. B_4C particles mainly locate at the boundary of aluminum crystals. Normalized matrix microstructure, avoiding particle distribution inhomogeneity, residual stress and the difference of grain size, will benefit to individually discuss the effect of interface microstructure on mechanical property of B_4C/Al composites.

Previous research has revealed that Ti atom tends to enrich at the Al-B_4C interface through equation (2) in the reaction system of B_4C, Al_3Ti and liquid aluminum. This reaction process concludes decomposition of Al_3Ti, corrosion of B_4C by aluminum melt and precipitation of TiB_2 on the B_4C surface [18]. Fig. 4 shows the distribution of B_4C particle and Ti element in prepared B_4C/Al composites. It is clear that Ti atoms obviously covered on the surface of B_4C particles. However, difference existed in the abundance degree of Ti element. In the matrix of C0.5, the Ti reaction layer was not continuous. Several B_4C particles' surface was even lacked of TiB_2 reaction product. However, with the increase of Ti content, TiB_2 reaction layer became more continuous and compact. As for the C2.5, Ti atoms were not only completely coated on the surface of B_4C particles, but also gathered in the aluminum matrix. Those enriched Ti atoms in Fig. 4 (d_2) corresponded to white spots in Fig. 4

(d_1), which were detached TiB_2 from Al-B_4C interface. Besides, the particle size of detached TiB_2 is much less than micrometer, which could possibly promote mechanical property of B_4C/Al composites as in situ nano-reinforcements.

Fig. 5 presents the interfacial microstructure of B_4C/Al composites with various Ti content. When the addition of Ti element was less at 0.5 wt.%, as shown in Fig. 5 (a)-(c), there existed many interface defects like micro-hole and cracks, although intact TiB_2 reactive layer was still formed. It should be noticed that TiB_2 layer was consisted of fine grain layer and dispersive coarse TiB_2 crystals. However, the Al-B_4C interface even detached from each other and formed server interface separation. When the addition of Ti element was increased to 1 wt.%, shown in Fig. 5 (d), the interface was modified that TiB_2 layer with more coarse TiB_2 crystals became continue and compact. Besides, although micro defects were generated, heavy interface separation was eliminated. If continuously increasing Ti content to 1.5 wt.%, intact interface reaction layer was obtained for all B_4C particles. The gradual improvement of interface combination between aluminum matrix and B_4C particle illustrates that adding Ti element into the melt promotes to modify interfacial microstructure and suppress the formation of defects. According to the interface microstructure change in Fig. 5, necessary Ti content for 15 wt.% B_4C should at least exceed 1.5 wt.%. Since B_4C powder was integrally added into the melt at one time, aggregated B_4C powder couldn’t be immediately scattered, considering the limited dispersion ability of mechanical stirrer. Thus, each B_4C particle didn’t participate in the interfacial reaction at the same time, instead, in a successive way. Those B_4C particles early contacting with liquid aluminum were more likely to generate intact TiB_2 layer through liquid diffusion reaction. However, if those B_4C particles didn’t react with melt in time, they intended to obtain weak interface bonding with matrix because of poor wetting between B_4C and liquid aluminum [25]. The number of covered B_4C particles by TiB_2 depends on the Ti content in melt. Sufficient Ti element will ensure all B_4C particles covered by a reaction layer finally. If Ti element is not enough, then various interface

microstructure like TiB_2 layer or interfacial defects will be formed.

For comparison, Fig. 6 presents the influence of high Ti content and long stirring time on interfacial microstructure. Due to severe interfacial reaction, interfacial microstructure contains reaction layer and many detached TiB_2 particles, and the former one is similar to the integral interface in Fig. 5, concluding continuous TiB_2 fine layer and discrete TiB_2 crystals. However, the morphology and distribution of these coarse TiB_2 crystals differ from that with lower Ti content. Many coarse TiB_2 crystals detached from B_4C surface and located near the interface or deeply into the aluminum matrix, as shown in Fig. 6b. During the stirring process, growth of TiB_2 crystals complied with nucleation and diffusion growth mechanism. The size of TiB_2 nucleus became larger along with stirring time. Due to strong shearing stress caused by flow field and growth mismatch stress, coarse TiB_2 crystals intended to deviate from growth site and flowed into the matrix by fluid melt. It is interested that two kinds of TiB_2 crystal morphology are observed: slice and needle-like. In fact, both morphologies are different section of hexagon TiB_2 crystal. Since diffusion Ti atoms were generated by the decomposition of Al_3Ti compound in the melt, preferential growth orientation of TiB_2 crystal directed to aluminum matrix. TiB_2 grew faster along with the matrix orientation owing to sufficient Ti atoms. TiB_2 with hexagon crystal structure was inclined to grow into 2D-hexagon slice, as shown in Fig. 6a. Therefore, the morphology of 2D-hexagon TiB_2 slice was similar to rod on the polished traverse surface. Except for white TiB_2 particles, there also exists few grey precipitation, which was proved to be AlB_2 in our previous research [17, 18]. It is promising that these nanoscale second precipitations TiB_2 will further strength the matrix and influence mechanical properties of B_4C/Al composites [26].

Typical tensile curves of stress versus strain for B_4C/Al composites are shown in Fig. 7 and the tested tensile properties are summarized in Table 2. It is clear that the reinforcement-matrix interfacial modification has an obvious effect on the tensile properties. Both average offset yield strength (0.2%) and ultimate tensile strength

basically become more and more large with enhanced Ti content, 46.4 MPa and 93.2 MPa for C0.5, however, 85.4 MPa and 139.8 MPa for C2.5, which illustrates that interfacial reaction promotes to strengthen the composites. But it should be noticed that the deformation ability is compromised, especially for C2.5 with a average ductility of 6.9%. Representative scanning electron micrographs of fracture surface at low magnification are presented in Fig. 8. Many toughening dimples with knife edges at the joint of the dimples and the wavy appearance of the serpentine glide on the dimple walls, caused by matrix slip lines intersecting the growing void, illustrates extensive void growth and a void coalescence mechanism by shear failure in the matrix between the voids. The dimples are essentially equiaxial and nearly uniform in size. However, the dimple size is much different if compared with each other. Most dimples in the matrix gradually became small with increasing Ti content. The surface morphology in Fig. 7d presents many fine dimples. These micro-dimples indicate the insufficient evolution of plastic deformation, which is consistent with the lower ductility exhibited by C2.5. Besides, it was also found that some B_4C particles with flat and smooth surfaces were located on the fracture surface, which proves that particles have been broken during the tensile process. Particles break-up indicates that effective load transfer happened through the interface, which is positive to the mechanical property of B_4C/Al composite [9, 13].

Fig. 9 shows interfacial fracture morphology of C0.5. There are basically two kinds of interfacial microstructure existing in the matrix, well-bonded interface and interfacial defects, concluding crack, hole and interfacial decohesion. Well-bonded interface was generated because of minor addition Ti. Due to the shortage of active Ti element, it was difficult for all particle surface covered by continuous and compact TiB_2 layer. Thus, various interface defects were formed in the matrix. These defects indicate that weak interface combination universally existed in the C0.5, in which crack propagation predominantly occurred by decohesion at the particle-matrix interface. Some B_4C reinforcements are only partially bonded to the matrix and still

have sharp edges and fragment surfaces, which are features of original B_4C particles in as-received condition. Due to the weak physical bonding between the B_4C particles and matrix, interface are the easier sites for crack generation and diffusion. Severe interface separation even occurred during the tensile process. These phenomena prove the poor mechanical behavior of C0.5. Fig. 10 presents the SEM images of interface microstructure of C1 and C1.5. With the increasing of Ti content, a different behavior was observed in other composites. More B_4C particles with flat and smooth surfaces are located on the fracture surface, which illustrates that particle breakage took place during the fracture process and is proof of a strong particle-matrix chemical bond. A continuous TiB_2 layer existed at the interface and jointed B_4C particles and aluminum matrix. Previous research have pointed out that the wetting angle between aluminum liquid and TiB_2 is much lower than that between liquid aluminum and B_4C. The former one is less than 90°, while the latter one is about 127°, showing apparent unwettable property [25, 27]. Improved wetting property eliminated typical interface defects and formed tight and chemical interface combination. Thus, load transfer through reaction interface could take place during the tensile test, and harder B_4C particles acted as reinforcements to strength the matrix and enhance the mechanical property of B_4C/Al composites.

The fracture surface of C2.5 with special morphology is shown in Fig. 11. Due to sufficient interface reaction, the C2.5 similarly generated continuous TiB_2 layer at the B_4C-Al interface. Fracture surface shows broken B_4C particles, which illustrates that load transfer occurred through TiB_2 layer. A worth notable morphology in Fig. 11a is the fine dimples near Al-B_4C interface, which are not produced on fracture surface of other B_4C/Al composites. Although the most strength was achieved for C2.5, its ductility decreased to a lower level, about 6.9%. This change could be explained by the fine dimples. From the EDS map in Fig. 11b, Ti element clearly enriched at the core of fine dimples. Considering the departed nanoscale TiB_2 particles, shown in Fig. 6, the Ti enrichment was aroused by departed TiB_2 particles. Fig. 11c presents a

higher magnification image of fine dimples. Some flake-like TiB_2 particles located at the center of fine dimples. These TiB_2 particles occupied dimple center and resulted in the formation of many fine dimples, which accounted for the smaller dimple size on the fracture surface of C2.5 with heavy interfacial reaction shown in Fig. 8. Smaller dimple size resulted in aluminium matrix limited deformation and thus lower ductility. However, the formation of nanoscale TiB_2 introduced many in situ second reinforcements into the composites. TiB_2 has nano-scale size and higher wettability with aluminium compared with B_4C particles, which effectively strengthened the matrix and increased tensile strength of B_4C/Al composites.

Considering the same recrystallized matrix, mass fraction and uniform distribution of B_4C particles, the results listed above illustrate that the mechanical property of B_4C/Al composite can be improved through interfacial modification. In second particles reinforced metal matrix composites, the contribution of reinforcements to mechanical property strongly depends on how closely the matrix and reinforcements combine [10]. Well bonded interface helps to effectively transfer loads to hardening particles, thus improves the strength of composite materials. On the contrary, if weak bonded interface or interfacial defects are formed, loads transfer will be impacted and thus the strength effect of reinforcement is limited [9]. In this experiment, the strength was gradually increased along with enhanced interfacial modification, which was related to the formation of TiB_2 nanolayer. Interfacial reaction made a chemical bonding between reinforcing particles and matrix, which was firmer compared with mechanical occlusion of physics surface. For the chemically bonded interface, a crystallographic orientation relationship is likely to exist on both sides of the interface. Interface bonding is continuous at an atomic level [13]. In this paper, TiB_2 layer made B_4C closely integrated with the Al matrix, and promoted effective load transfer.

The interfacial TiB_2 layer has also changed the fracture behavior of B_4C/Al composites. The fracture morphology presented in Fig. 9 to 11 displays a clear

difference between B_4C particles coated with TiB_2 layer and without. The former ones mainly failed in the form of reinforcement breakage; however, the later ones, with interfacial defects, failed in the form of interface departure, and B_4C particles were unbroken. The mechanism of two kinds of fracture behaviors is essentially a competitive relation between interface strength and reinforcement strength. Due to stress concentration at interfacial area, load is transferred to the B_4C particles. If the strength of interface is greater than that of reinforcement, fracture will give priority to particle broken; if the strength of interface is lower than that of reinforcement, interface failure is easier to happen. Different failure modes presented above indicate that TiB_2 layer strongly improved interfacial bonding strength in a way of B_4C particles breakage.

Although interfacial modification improved the strength, plastic deformation was decreased for B_4C/Al composites, especially with heavy interfical modification. For metal matrix composites, with increase of volume fraction of reinforcements, the strength usually increases and elongation decreases [10]. In this experiment, the interfacial TiB_2 layer made B_4C particles effectively participate in the loading process; while interface defects hindered B_4C particles to bear stress. Due to the contribution to strength and constraint on matrix plastic deformation mainly from the first kind of B_4C particles, the fraction of this kind of B_4C particles is named valid volume fraction of B_4C/Al composites. M. Kouzeli et.al confirmed that mechanical behavior of composite materials was related to the average distance between reinforcements [28]. The average distance is defined by equation (3):

$$\lambda = (1 - V_p)/N_L \tag{3}$$

where V_p is the volume fraction of particles, N_L is defined as the intersection of particle number per unit length of straight line on SEM map of B_4C/Al composites. With the improvement of interface reaction, the valid volume fraction V_p of reinforcements increased, and thus the average distance λ of particles decreased. For C2.5, interfacial reaction generated lots of nanoscale second phase TiB_2. These fallen

TiB_2 increased the volume fraction of total reinforcement fraction, leading to further decrease of particle distance N_L. The decrease of the particle spacing means smaller unit matrix plastic deformation of micro area, which on the one hand caused a higher flow stress during deformation and increased yield and tensile strength; On the other hand, resulted that pores aggregation was not fully developed. Therefore, the ability of plastic deformation was reduced and elongation was decreased.

Conclusion

Through the microstructure characterization and mechanical test of B_4C/Al composite materials with different degree of interfical modification, the effect of interfacial reaction on mechanical behavior was revealed. Main conclusions are the following:

1. The addition of Ti elements into the matrix help to form TiB_2 chemical-bonding interface through interfacial reaction. When the content of Ti was over much, which was about 1.5 wt.% for 15 wt% B_4C particles, the surfaces of B_4C were covered by fine, continuous and dense TiB_2 layer. Thus B_4C-Al interface obtained strong bonding. However, when Ti content was insufficient, lots of interfacial defects were unavoidably formed.

2. The surface modification on B_4C through regulating the interfacial structure affected mechanical properties of B_4C/Al composites. As the degree of interfacial reaction increased, B_4C/Al composites with more fine TiB_2 layer presented higher yield strength and tensile strength, but the elongation was reduced.

3. The fracture surface of B_4C/Al composites with toughening dimples indicates that fracture behavior was given priority to a void coalescence mechanism. The TiB_2 layer eliminated the interfacial defects, and made an effective load transfer process, thus improved the strength. The coarse TiB2 particles generated by interfacial reaction further strengthened the matrix as in situ second reinforcement, but also resulted in smaller toughening dimples and thus lower ductility.

Acknowledge

The authors thank the financial support from China Nuclear Power Engineering Co., Ltd. under grant No. 2013966003.

References

[1] F. Thevenot, Boron carbide-a comprehensive review, J. Eur. Ceram. Soc. 6 (1990) 205-225.

[2] G. Bonnet, V. Rohr, X.G. Chen, J.L. Bernier, R. Chiocca, H. Issard, Use of Alcan's Al-B_4C metal matrix composites as neutron absorber material in TN International's transportation and storage casks, Packaging, Transport, Storage & Security of Radioactive Material 20 (2009) 98-102.

[3] P. Zhang, Y. Li, W. Wang, Z. Gao, B. Wang, The design, fabrication and properties of B_4C/Al neutron absorbers, J. Nucl. Mater. 437 (2013) 350-358.

[4] Handbook of neutron absorber materials for spent fuel transportation and storage application: 2009 edition. EPRI, Palo Alto CA: 2009. 1019110.

[5] T.W. Clyne, P.J. Withers, An introduction to metal matrix composites, New York: Cambridge Univ. Press, 1993.

[6] Y. Li, K.T. Ramesh, Influence of particle volume fraction, shape, and aspect ratio on the behavior of particle-reinforced metal-matrix composites at high rates of strain, Acta Mater. 46 (1998) 5633-5646.

[7] M. Kouzeli, A. Mortensen, Size dependent strengthening in particle reinforced aluminium, Acta Mater. 50 (2002) 39-51.

[8] J.E. Spowart, D.B. Miracle, The influence of reinforcement morphology on the tensile response of 6061/SiC/25p discontinuously-reinforced aluminum, Mater. Sci. Eng. A 357 (2003) 111-123.

[9] J. Song, Q. Guo, Q. Ouyang, Y. Su, J. Zhang, E.J. Lavernia, J.M. Schoenung, D. Zhang, Influence of interfaces on the mechanical behavior of SiC particulate-reinforced Al–Zn–Mg–Cu composites, Mater. Sci. Eng. A 644 (2015) 79-84.

[10] N. Chawla, Y.L. Shen, Mechanical behavior of particle reinforced metal matrix composites, Adv. Eng. Mater. 3 (2001) 357-370.

[11] H. Zhang, K. Ramesh, E. Chin, Effects of interfacial debonding on the rate-dependent response of metal matrix composites, Acta Mater. 53 (2005) 4687-4700.

[12] H. Zhang, M.W. Chen, K.T. Ramesh, J. Ye, J.M. Schoenung, E.S.C. Chin, Tensile behavior and dynamic failure of aluminum 6092/B_4C composites, Mater. Sci. Eng. A 433 (2006) 70-82.

[13] L.M. Tham, M. Gupta, L. Cheng, Effect of limited matrix-reinforcement interfacial reaction on enhancing the mechanical properties of aluminium-silicon carbide composites, Acta Mater. 49 (2001) 3243-3253.

[14] L.M. Tham, M. Gupta, L. Cheng, Predicting the failure strains of Al/SiC composites with reacted matrix-reinforcement interfaces, Mater. Sci. Eng. A 354 (2003) 369-376.

[15] D.J. Lloyd, Aspects of fracture in particulate reinforced matrix composite, Acta Metall. Mater. 39 (1991) 59-71.

[16] Z. Zhang, X.G. Chen, A. Charette, Particle distribution and interfacial reactions of Al-7%Si-10%B_4C die casting composite, J. Mater. Sci. 42 (2007) 7354-7362.

[17] J.C. Viala, J. Bouix, G. Gonzalez, C. Esnouf, Chemical reactivity of aluminium with boron carbide, J. Mater. Sci. 32 (1997) 4559-4573.

[18] J. Zheng, Q. Li, W. Liu, G. Shu, Microstructure evolution of 15 wt% boron carbide/aluminum composites during liquid-stirring process, J. Compos. Mater. 50 (2016) 3843-3852.

[19] Z. Zhang, K. Fortin, A. Charette, X.G. Chen, Effect of titanium on microstructure and fluidity of Al-B_4C composites, J. Mater. Sci. 46 (2011) 3176-3185.

[20] A.R. Kennedy, B. Brampton, The reactive wetting and incorporation of B_4C particles into molten aluminium, Scripta Mater. 44 (2001) 1077-1082.

[21] E.A. Feest, Interfacial phenomena in metal-matrix composites, Composites 25

(1994) 75-86.

[22] A.R. Kennedy, The microstructure and mechanical properties of Al-Si-B_4C metal matrix composites, J. Mater. Sci. 37 (2002) 317-323.

[23] Z. Luo, Y. Song, S. Zhang, D.J. Miller, Interfacial microstructure in a B_4C/Al Composite Fabricated by Pressureless Infiltration, Metall. Mater. Trans. A 43 (2012) 281-293.

[24] C. Garcia-Cordovilla, E. Louis, J. Narciso, Pressure infiltration of packed ceramic particulates by liquid metals, Acta Mater. 47 (1999) 4461-4479.

[25] D. Kocaefe, A. Sarkar, X. Chen, Effect of Ti addition on the wettability of Al-B_4C metal matrix composites, Int. J. Mater. Res. 103 (2012) 729-736.

[26] L. Lü, M.O. Lai, Y. Su, H.L. Teo, C.F. Feng, In situ TiB_2 reinforced Al alloy composites, Scripta Mater. 45 (2001) 1017-1023.

[27] Q. Lin, P. Shen, F. Qiu, D. Zhang, Q. Jiang, Wetting of polycrystalline B_4C by molten Al at 1173-1473K, Scripta Mater. 60 (2009) 960-963.

[28] M. Kouzeli, A. Mortensen, Size dependent strengthening in particle reinforced aluminium, Acta Mater. 50 (2002) 39-51.

Captions

Table 1 Experimental parameters for B_4C/Al composites billets during stirring process.

Fig. 1. The size of tensile specimen of B_4C/Al composites (mm).

Fig. 2. Particle distribution of B_4C/Al composites under different preparation conditions, (a) C0.5，(b) C1，(c) C1.5，and (d) C2.5. The white particle in picture (c) is Al_3Ti.

Fig. 3. EBSD pictures of recrystallization annealed B_4C/Al composites: (a) C0.5, (b) C1，(c) C1.5，and (d) C2.5.

Fig. 4. BSE images of B_4C/Al composites under different Ti content and stirring time: (a_1) C0.5，(b_1) C1，(c_1) C1.5，and (d_1) C2.5. Images (a_2)-(d_2) are corresponding distribution of Ti element recorded by EDS.

Fig. 5. SEM images of interfacial microstructure in B_4C/Al composites with different processing parameters: (a)-(c) C0.5, (b) C1.0 and (c) C1.5.

Fig. 6. Interfacial microstructure of C2.5, (a) interfacial reaction layer and (b) second reaction products in the matrix.

Fig. 7. Typical tensile stress versus strain curves for the B_4C/Al composites with different interface modification conditions.

Table 2 Tensile properties of the B_4C/Al composites.

Fig. 8. SEM pictures of fracture surface morphology of B_4C/Al composites: (a) C0.5, (b) C1, (c) C1.5, and (d) C2.5.

Fig. 9. Fracture surface of C0.5 with different interfacial microstructure showing: (a) reaction bonding interface, (b) crack, (c) hole and (d) interface separation. The inserted pictures are high magnification of corresponding areas.

Fig. 10. SEM images of presentable interface microstructure for B_4C/Al composites: (a) C1 and (b) C1.5.

Fig. 11. Fracture surface of C2.5 presenting special morphology: (a) reaction layer TiB_2 and fine dimples, (b) EDS map of Ti element in (a), and (c) higher magnification

image of the fine dimples.

Fig. 1.

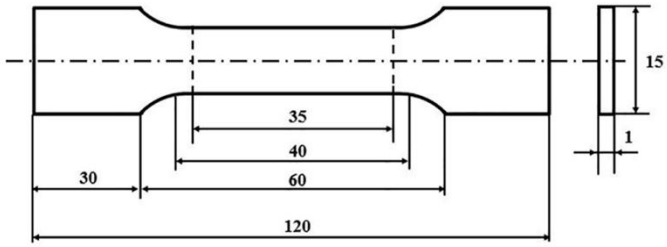

Single column

Fig. 2.

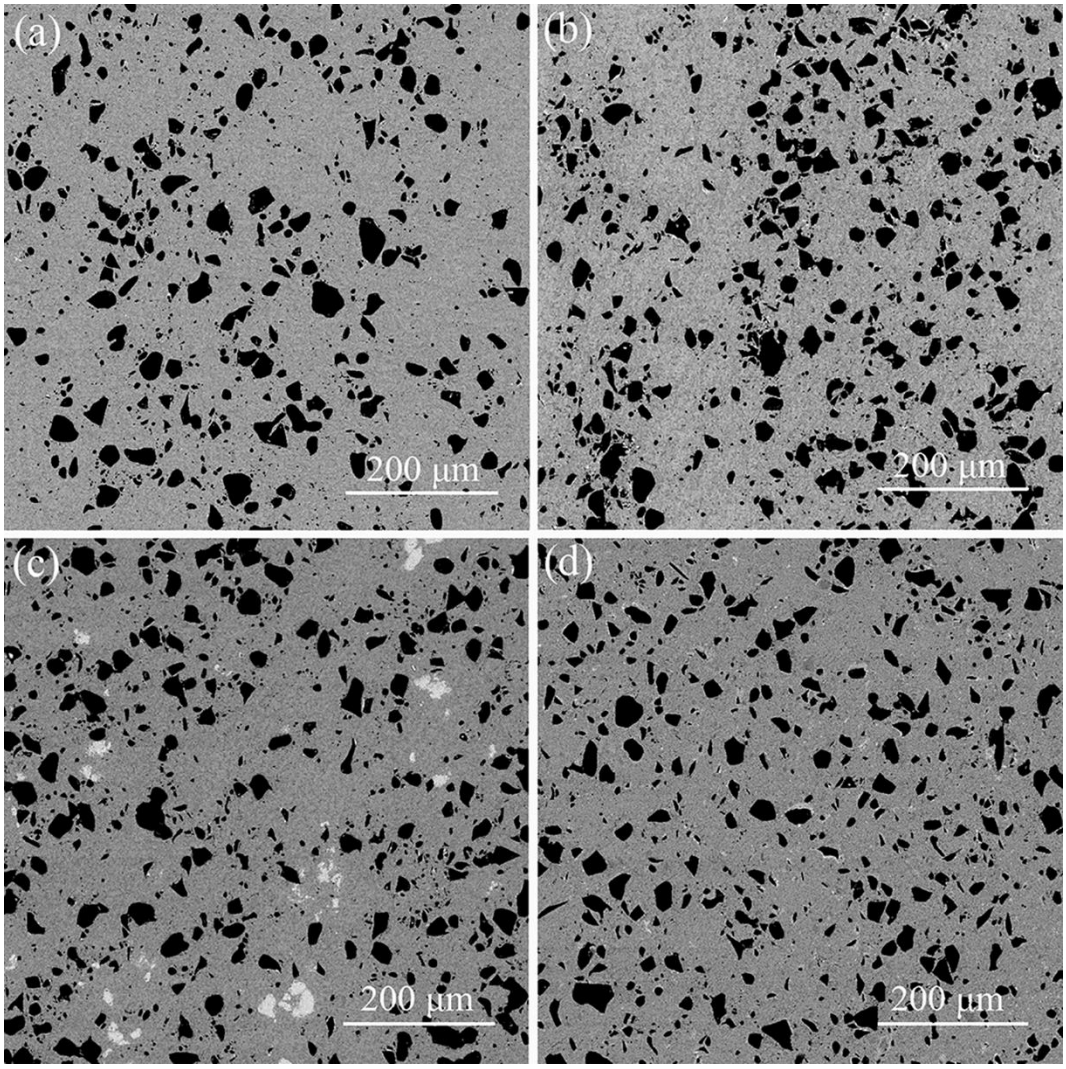

1.5 column

Fig. 3.

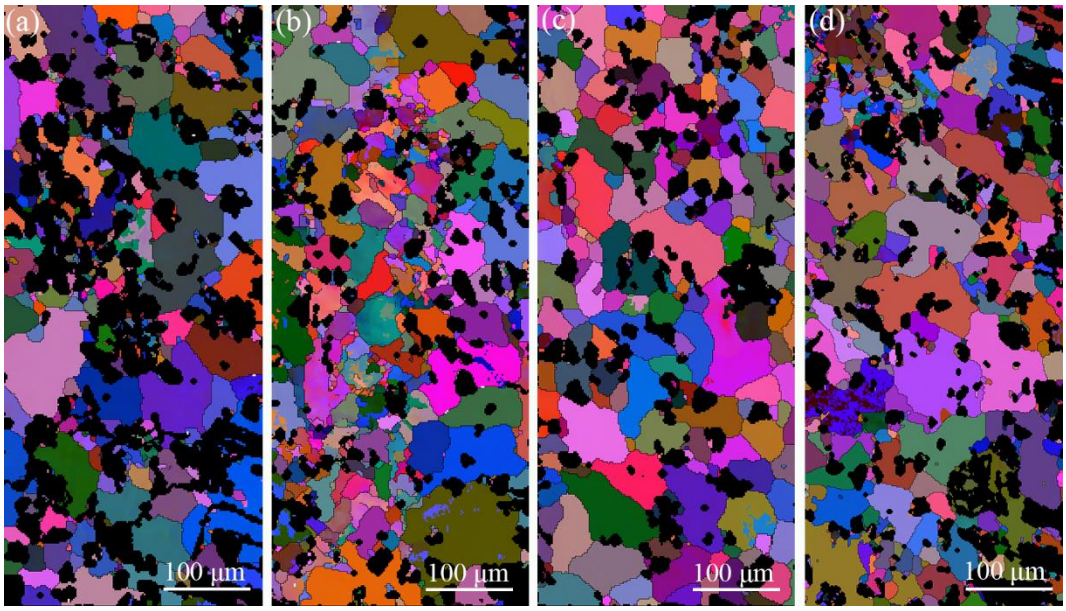

1.5 column

Fig. 4.

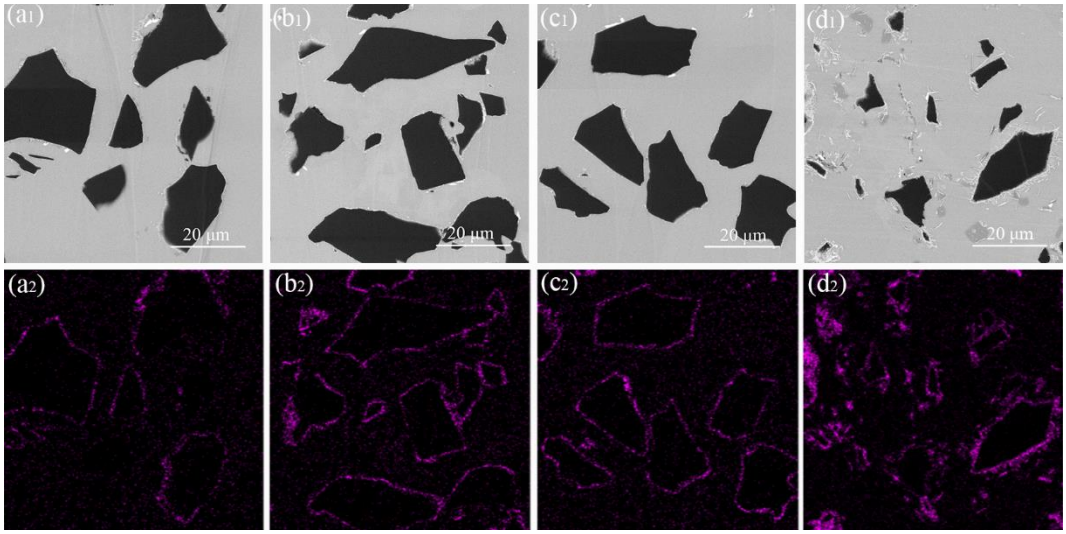

1.5 column

Fig. 5.

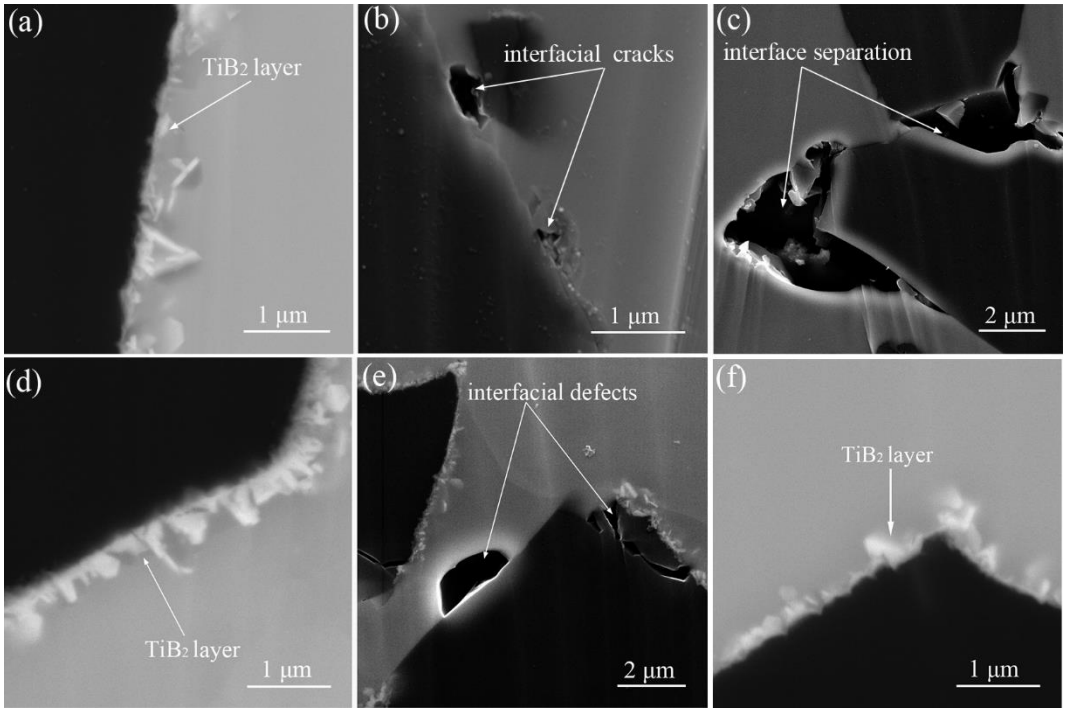

1.5 column

Fig. 6.

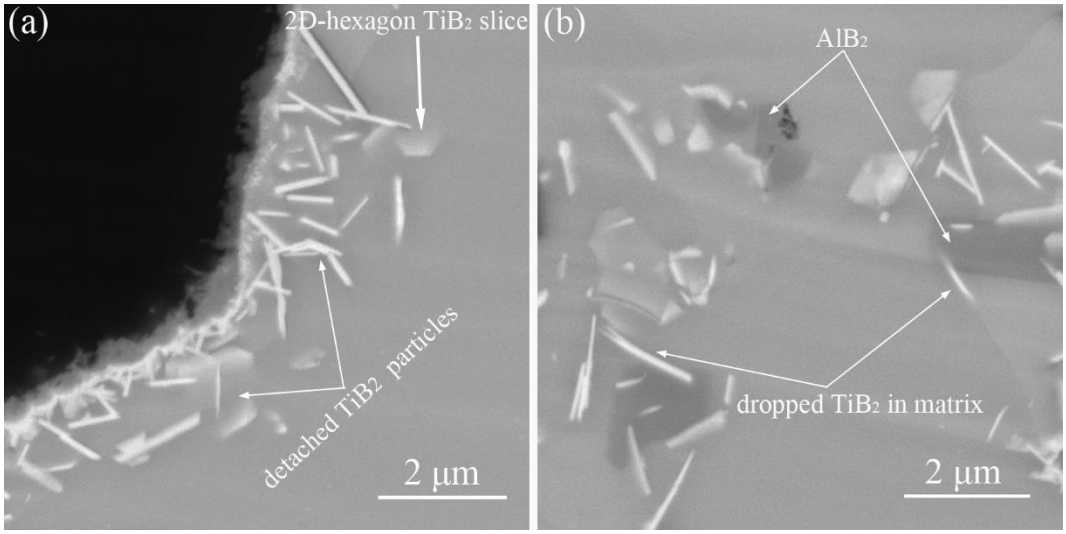

1.5 column

Fig. 7.

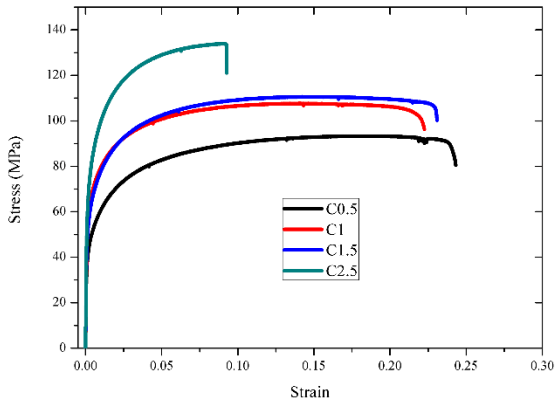

Single column

Fig. 8.

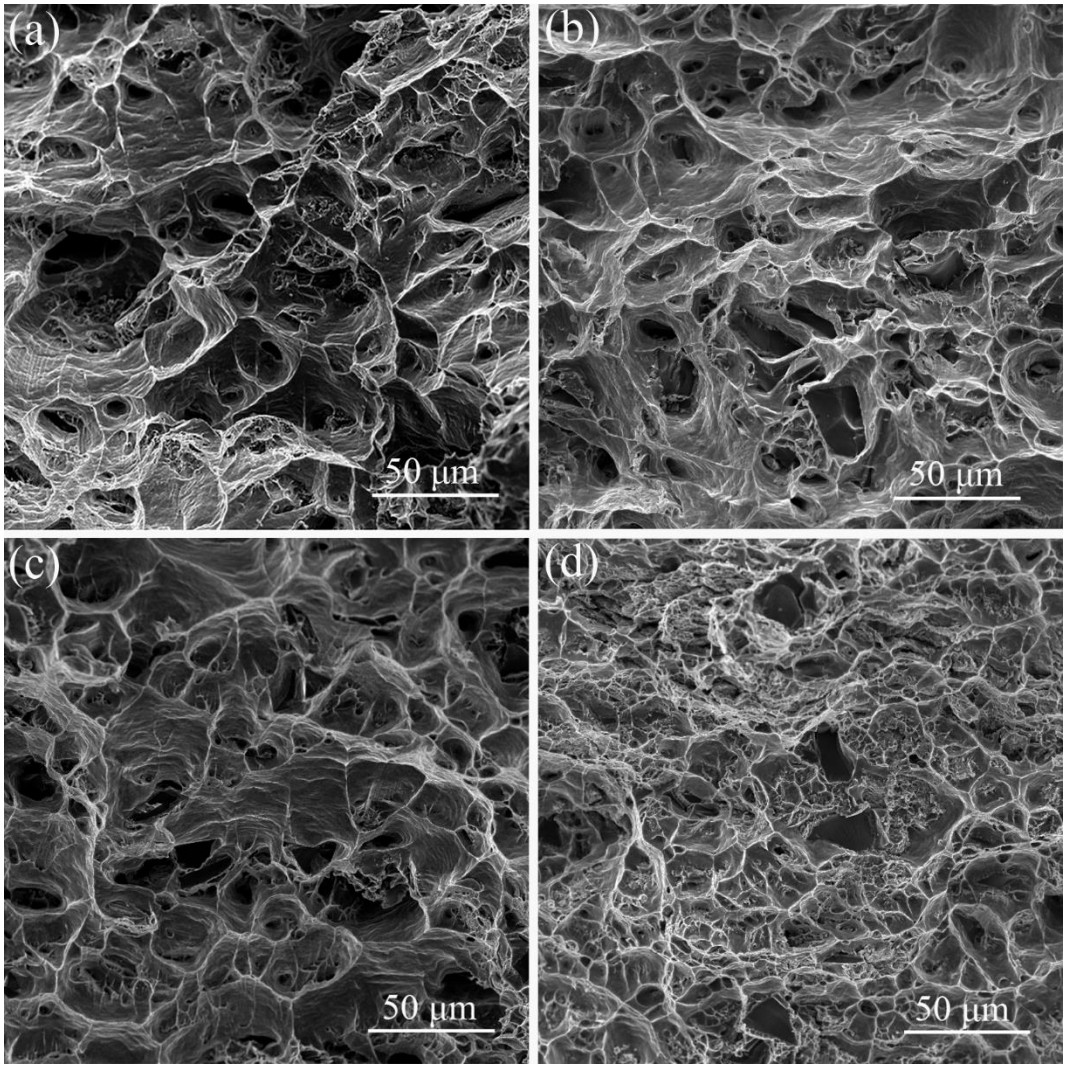

1.5 column

Fig. 9.

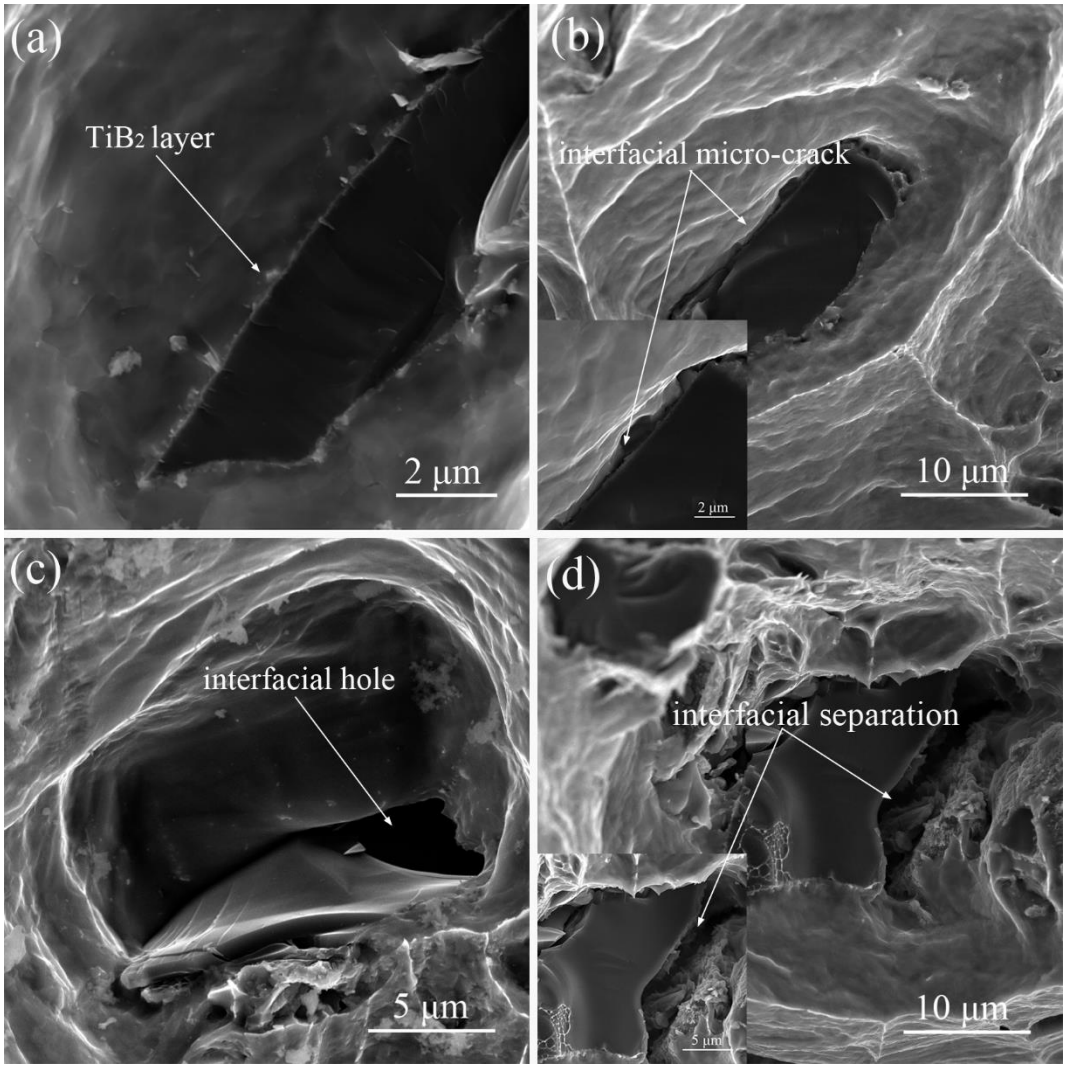

1.5 column

Fig. 10.

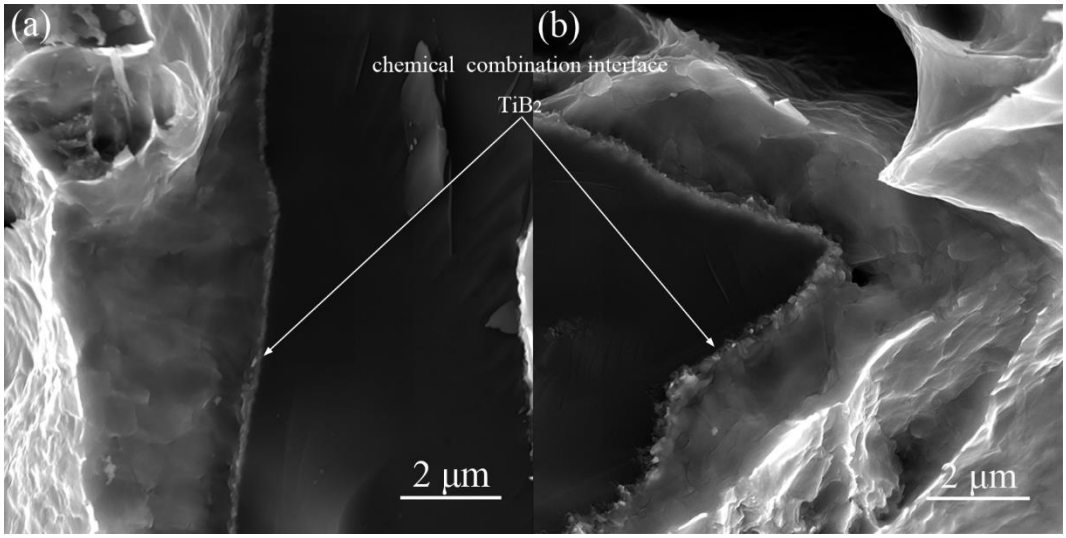

1.5 column

Fig. 11.

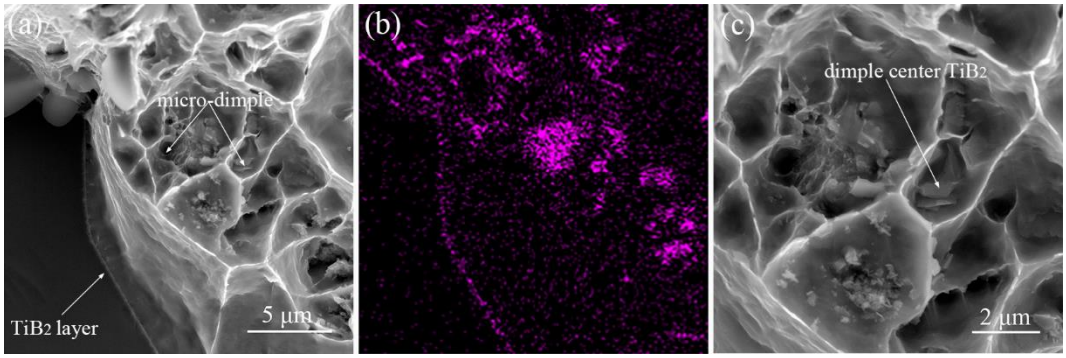

1.5 column

Table 1

Serial number of billets	1	2	3	4
Ti (wt.%)	0.5	1	1.5	2.5
Stirirng time (min)	10	10	10	55
IDs	C0.5	C1	C1.5	C2.5

Single column

Table 2

	C0.5	C1	C1.5	C2.5
$\sigma_{0.2\%}$ (MPa)	46.4 ±0.3	69.4 ±6.4	60.6 ±0.5	85.4 ±6.6
σ_b (MPa)	93.2 ±1.0	110.6 ±1.8	111.1 ±0.5	138.9 ±6.2
δ (%)	27.1 ±1.6	19.8 ±2.1	19.1 ±2.8	6.9 ±1.5

$\sigma_{0.2\%}$: offset yield strength at 0.2% strain; σ_b: ultimate tensile strength; δ: ductility.

Single column